Enhanced seismic imaging in the Midland Basin with multiparameter full-waveform inversion

James Sheng[1]*, Guanghui Huang[1], Terence Krishnasamy[1], Andrew Peterson[1], Jaime Ramos-Martínez[1] and Carlos Calderón-Macías[1] introduce a multiparameter full-waveform inversion (FWI) approach for land seismic imaging that jointly estimates subsurface velocity and reflectivity.

Abstract

We introduce a multiparameter full-waveform inversion (FWI) approach for land seismic imaging that jointly estimates subsurface velocity and reflectivity. The method employs a scale-separation strategy to recover background velocity and high-resolution reflectivity, extending imaging beyond the depth limits of head and diving waves. To enhance robustness against noise and low-frequency limitations, we incorporate a dynamic matching objective function that aligns observed and modelled phases through multidimensional correlation, reducing sensitivity to amplitude mismatches and low signal-to-noise ratios. The reflectivity kernel further improves high-wavenumber content, delivering superior resolution and structural coherence compared to conventional imaging. Application to a Midland Basin land dataset demonstrates the method's potential for high-resolution imaging in complex geological settings.

Introduction

Full-waveform inversion (FWI) has become a powerful tool for high-resolution subsurface imaging, but its application in land environments remains challenging compared to marine settings. Key difficulties include low signal-to-noise ratios (SNR) at low frequencies, uncertainties in source wavelet estimation, and the strong influence of surface topography. For shallow imaging, limited near-offset coverage and complex near-surface geology often obscure primary reflections required by conventional seismic imaging approaches (e.g., Reta-Tang et al., 2023).

To overcome these limitations, leveraging the full wavefield, including refracted and multi-scattered energy, can improve subsurface illumination and velocity model building. Refracted waves provide essential constraints for velocity estimation, but their penetration depth is restricted by acquisition geometry. Beyond this limit, or in zones of velocity reversal, reflected energy becomes the primary source of information for updating the velocity model.

In this work, we present a multiparameter FWI (MP-FWI) approach that jointly estimates P-wave velocity and reflectivity, addressing several of the challenges outlined above. This methodology was first introduced for acoustic media by Yang et al. (2021) and later extended to elastic cases by Huang et al. (2025). Here, we adopt the acoustic implementation and combine it with the dynamic matching (DM) objective function (Huang et al., 2021) to enhance robustness against noise and amplitude mismatches. We describe the method and demonstrate its effectiveness using a land seismic dataset from the Midland Basin, targeting formations such as the Barnett Shale and Mississippi Limes.

MP-FWI for P-Wave velocity and reflectivity

Our multiparameter full-waveform inversion (MP-FWI) implementation jointly estimates P-wave velocity and reflectivity through two key components:

(i) a wave-equation parameterisation in terms of P-wave velocity and reflectivity, and
(ii) a scale-separation algorithm applied to the FWI gradient to minimise crosstalk between these parameters.

Using reflectivity in the acoustic wave-equation parameterisation eliminates the need to estimate density for synthesizing reflected events, which is advantageous given the difficulty of recovering density from surface seismic data. This formulation also enables simulation of the full acoustic wavefield from a single equation, unlike Born-based implementations. Consequently, multi-scattering, free-surface multiples, and refracted arrivals are naturally incorporated into the inversion (Whitmore et al., 2020).

The scale-separation strategy, grounded in inverse scattering theory, decomposes the FWI gradient into two sensitivity kernels: a long-wavelength kernel for velocity updates (Ramos-Martinez et al., 2016) and a high-wavenumber kernel for reflectivity updates (Whitmore and Crawley, 2012). This decomposition improves robustness and effectiveness when jointly inverting for velocity and reflectivity.

Although recent land surveys have adopted longer offsets (e.g., Kumar et al., 2025), they remain shorter than those in ocean-bottom node (OBN) acquisitions, limiting refracted-wave penetration depth. Beyond this depth, velocity updates rely primarily on reflected energy, with the sensitivity kernel used by our MP-FWI approach, emphasising background velocity adjustments. For shallow targets, this velocity kernel mitigates high-wavenumber leakage in velocity updates caused by reflection interference.

[1] TGS
* Corresponding author, E-mail: james.sheng@tgs.com
DOI: 10.3997/1365-2397.fb2026008

Parameter	Value
Nominal shot-line interval	202 m
Nominal receiver-line interval	202 m
Nominal shot interval	25 m
Nominal receiver interval	50 m
Patch size	240 × 16 channels
Maximum nominal offset	8000 m

Table 1 Acquisition parameters for the study area.

To enhance low-frequency velocity estimation, we incorporate the dynamic matching (DM) objective function. DM-FWI uses multidimensional cross-correlation to quantify time-dependent mismatches between observed and synthetic data (Mao et al., 2020; Huang et al., 2023). By maximising phase alignment, DM reduces the impact of amplitude discrepancies and low SNR conditions — critical for land FWI applications (Reta-Tang et al., 2023; Krishnasamy et al., 2023).

For reflectivity inversion, multi-scattering improves shallow subsurface illumination beyond what primary reflections provide. The reflectivity kernel emphasises high-wavenumber content, and iterative updating reconstructs relative amplitudes, enhancing resolution and structural coherence. Likewise, multiple attenuation can be automatically addressed during the iterative inversion as the waveform match is improved.

Field data example

The study area corresponds to an onshore seismic survey acquired in the Midland Basin, a sub-basin of the Permian Basin, near Odessa, Texas, USA (Figure 1). The survey was designed to support evaluation and development of multiple prospective zones, including the Barnett Shale, Mississippi Lime, and Devonian horizons (e.g., Sutton et al., 2005). Acquisition employed Vibroseis sources with a low-dwell sweep ranging from 2 to 94 Hz. Table 1 summarises the main acquisition parameters.

Initial near-surface model and preprocessing

Preconditioning the seismic data prior to FWI is critical, particularly for land surveys where low-frequency signal-to-noise ratios (SNR) are often poor. The goal is to suppress energy that cannot

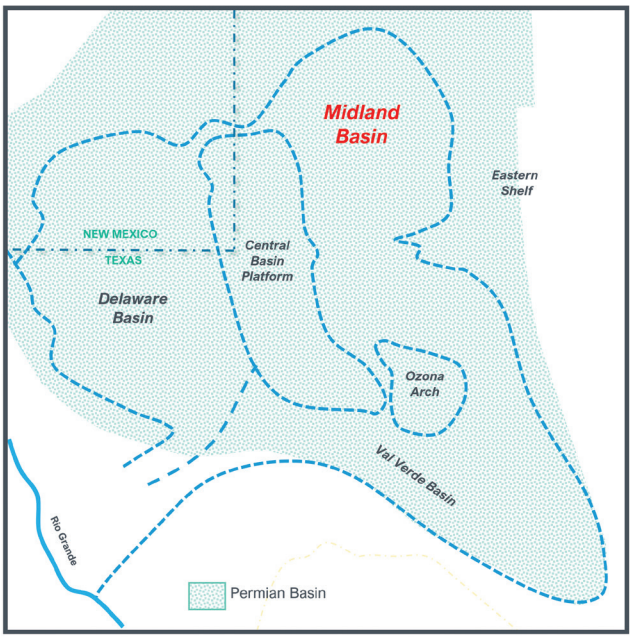

Modified from S. Dutton et al., 2005

Figure 1 Study area location in the Midland Basin relative to the larger Permian Basin (modified from S. Dutton et al., 2005)

be reproduced by acoustic forward modelling, thereby improving inversion stability and reliability. The preprocessing workflow includes:

- Harmonic-noise attenuation
- Minimum-phase conversion
- Low-frequency geophone-response compensation
- High-amplitude noise suppression
- Linear and ground-roll attenuation
- Inverse-Q compensation

Figure 2 shows example shot records filtered to 8 Hz before and after preconditioning. Despite these efforts, the usable starting frequency for FWI remains constrained to approximately 5 Hz due to spatially variable SNR.

No static corrections — neither conventional nor residual — were applied to the data used in the FWI workflow. This choice ensures that inversion remains sensitive to near-surface velocity anomalies rather than being influenced by externally imposed shifts (Krishnasamy et al., 2025).

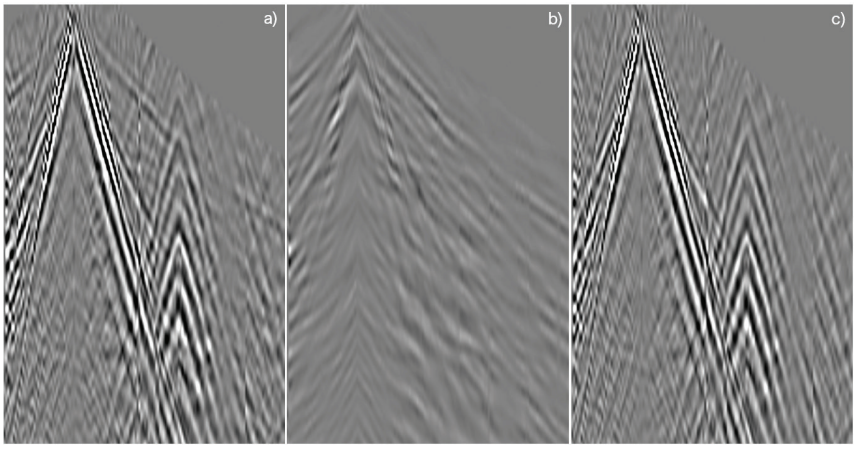

Figure 2 Sample recorded shot gather filtered with a maximum corner frequency of 8 Hz; a) before pre-processing b) after pre-processing and c) noise removed.

Velocity model-building

The initial near-surface model was constructed using refraction tomography, supplemented where possible by shallow sonic logs (Figure 3a). FWI began at 5 Hz using the dynamic matching (DM) objective function, initially focusing on refracted waves. A multi-scale approach was adopted, progressively increasing frequency and offset ranges at each stage. Additionally, a data-domain quality factor was applied to down-weight low-SNR contributions, reducing noise influence and improving inversion reliability. Refracted-energy penetration is limited by available offsets; beyond this depth, multi-azimuth reflection tomography is typically employed to update deeper velocity.

With this updated model (Figure 3b), velocity refinement continued using MP-FWI with reflectivity. At this stage, additional data conditioning was applied to improve waveform matching, including surface-consistent deconvolution, further noise attenuation in multiple domains, and several passes of surface-consistent scaling. Reparametrising the wave equation in terms of velocity and reflectivity enables reflectivity-driven updates beyond refracted-wave penetration depth within the same inversion framework. Scale separation in the FWI gradient provides a velocity kernel for updating background velocity (Figure 4). Starting from the initial model (Figure 3b), velocity updates using the conventional FWI gradient (Figure 4a) are compared to those using the velocity kernel (Figure 4b). Conventional updates exhibit high-wavenumber features from specular reflections — typically an order of magnitude larger than tomographic updates — requiring additional conditioning and reflection tomography in

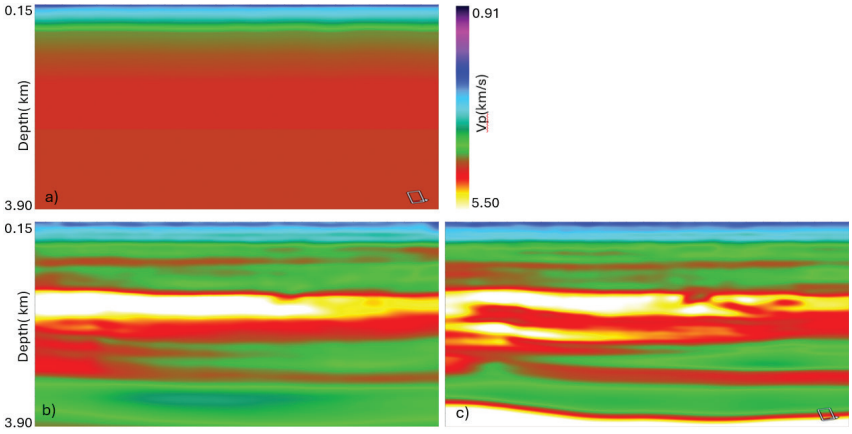

Figure 3 a) Initial velocity model; b) intermediate velocity used for MP-FWI c) final MP-FWI velocity model.

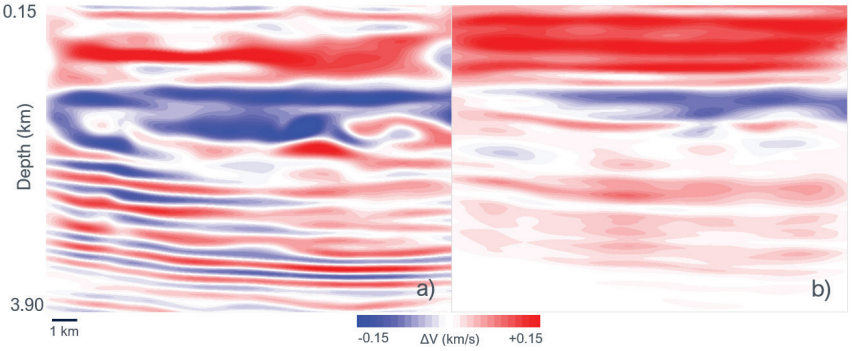

Figure 4 Velocity updates at one stage departing from starting velocity model (Figure 3b) using a) the conventional FWI gradient and b) the MP-FWI velocity kernel. A strong migration imprint is present in the conventional FWI update, which prevents background velocity updates with reflected energy.

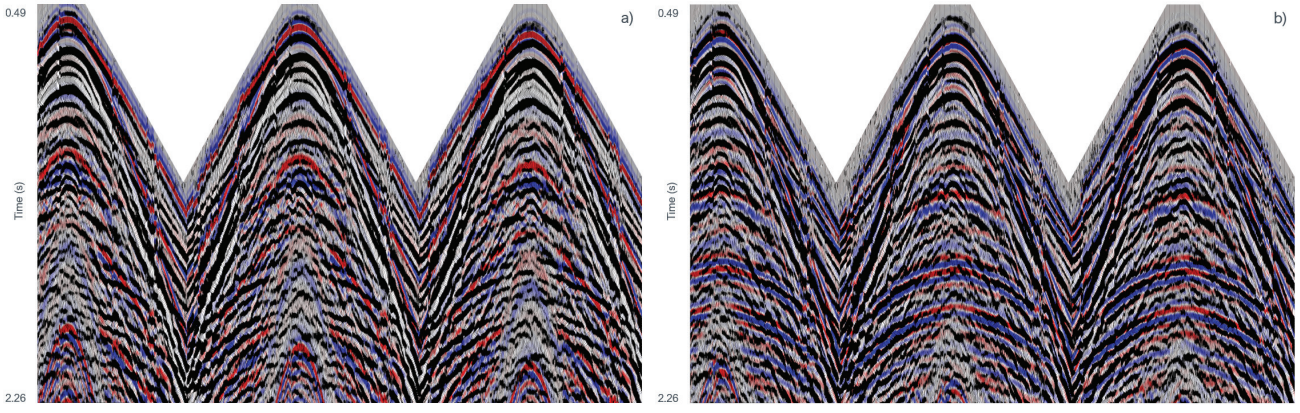

Figure 5 Comparison of field (wiggles) and synthetic (colour) shot gathers. Synthetic shot gathers were computed from a) initial and b) updated velocity model; For a perfect velocity model, the positive amplitudes of the synthetic, red, should be aligned with the positive amplitude, peaks, in the observed data and the negative amplitude of the synthetic, blue, should be aligned with the negative amplitude, troughs, on the observed data.

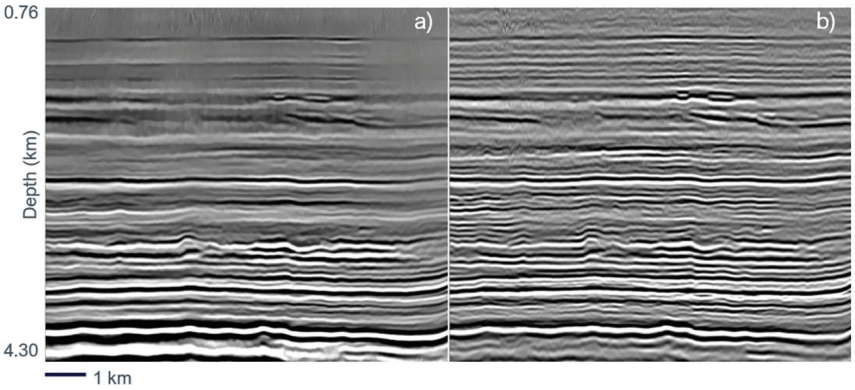

Figure 6 a) RTM and b) MP-FWI image along north-south direction.

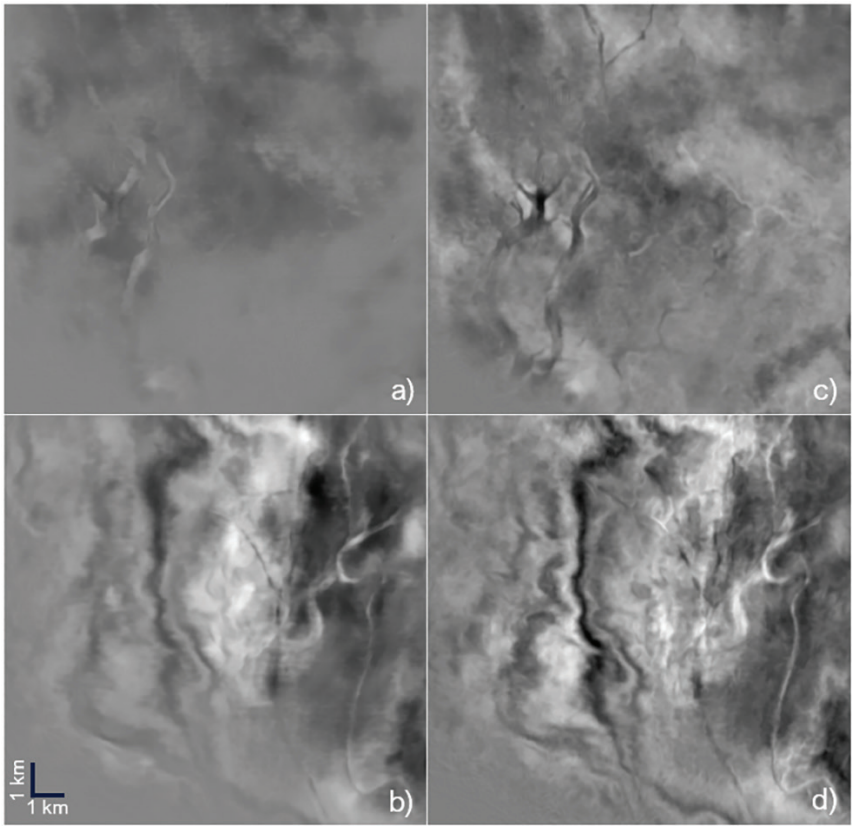

Figure 7 a), b) RTM images at depths 1.5 and 3.4 km, respectively; c), d) MP-FWII images for the same depths.

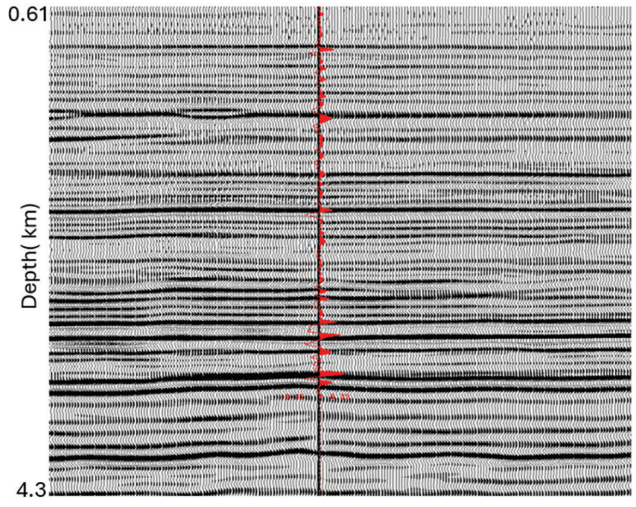

Figure 8 Comparison of the final reflectivity (wiggles) around a well location with the synthetic trace (red wiggle) computed from well logs.

standard workflows. In contrast, updates from the velocity kernel enhance low-wavenumber components, improving background velocity convergence within the same FWI framework. Once the background velocity is refined, higher-resolution updates can be achieved using the conventional gradient. The final background velocity model is shown in Figure 3c.

Model validation was performed by comparing synthetic common-receiver gathers for the initial (Figure 5a) and final (Figure 5b) velocity models with recorded data. Positive amplitudes in the recorded data (black) show improved alignment with positive amplitudes in the synthetic data (red) for the final model.

Imaging results

MP-FWI provides significant imaging benefits compared to conventional algorithms. Figure 6 compares crossline sections from MP-FWI (Figure 6b) and reverse-time migration (RTM) (Figure 6a), both computed from the final velocity model. MP-FWI delivers superior focusing and resolution, achieved through scale

separation that emphasises high-wavenumber features in reflectivity while reducing backscattering at high-impedance contrasts. Figure 7 shows similar comparisons for slices at depths of 1494 m and 3408 m, where channel definition in MP-FWI images is markedly improved over RTM. Finally, in Figure 8 we show a comparison of reflectivity at a well location with the synthetic trace computed from well information. As observed, there is good match of primary reflectors.

Conclusions

We have demonstrated the advantages of applying acoustic multiparameter full-waveform inversion (MP-FWI) for simultaneous velocity and reflectivity estimation using land seismic data from the Midland Basin, USA. Incorporating the dynamic matching (DM) objective function significantly enhances velocity estimation at low frequencies, where land data typically suffer from poor signal-to-noise ratios. The velocity kernel derived from scale separation enables reliable updates at depths where only reflected energy is available, improving convergence of the background velocity model. Reformulating the wave equation in terms of velocity and reflectivity eliminates the need for density estimation to generate synthetic reflectivity, simplifying the inversion process. Additionally, the reflectivity kernel facilitates iterative image reconstruction, delivering higher resolution, and improved continuity compared to conventional imaging approaches.

Acknowledgements

We thank TGS for authorising the publication of this work and TGS Multiclient for providing the dataset. We thank our colleagues in R&D Geophysics for the fruitful discussions that contributed to improving this work.

References

Dutton, S.P., Kim, E.M., Broadhead, R.F., Raatz, W.D., Breton, C.L., Ruppel, S.C and Kerans, C. [2005]. Play analysis and leading-edge oil-reservoir development methods in the Permian basin: Increased recovery through advanced technologies. *AAPG Bulletin,* ***89***, 553-576.

Huang, G., Macesanu, C., Liu, F., Ramos-Martinez, J., Whitmore, D., Calderon, C. and Bloor, R. [2025]. Multiparameter elastic FWI for joint inversion of velocity and reflectivity. 86th EAGE Annual Conference and Exhibition, *Extended Abstracts*.

Huang, Y., Mao J., Sheng, J., Perz, M, He, Y., Hao, F., Liu, F., Yong, S.L., Chaikin, D, Ramirez, A., Hart, M. and Roende, H. [2023]. Towards high-fidelity imaging: Dynamic Matching FWI. *The Leading Edge*, **42**, 124-132.

Krishnasamy, T., Beck, J. and Reta-Tang, C. [2025]. From statics to dynamics: enhancing onshore velocity models with full waveform inversion. *First Break*, **43**(1), 63-68.

Krishnasamy, T., Sheng, J., Florendo, R., Beck, J., Sierra, A., Murphy, S., Siebens, J. and Iwo-Brown, Y. [2023]. High-resolution near-surface land FWI across the Delaware basin fill zone. 3rd International Meeting for Applied Geoscience & Energy, *Expanded Abstracts*.

Mao, J., Sheng, J. and Hilburn, G. [2019]. Phase only reflection full-waveform inversion for high resolution model update. 89th SEG Annual International Meeting, *Expanded Abstracts*, 1305–1309.

Ramos-Martinez, J., Crawley, S., Zou, K., Valenciano, A.A., Qiu, L. and Chemingui, N. [2016]. A robust gradient for long wavelength FWI updates. 78th EAGE Annual Conference & Exhibition, *Extended Abstracts*.

Reta-Tang, C., Sheng, J., Liu, F., Vazquez, A. and Cabrera, A. [2023]. Applications of full waveform inversion to land data: case studies in onshore Mexico. *The Leading Edge*, **42**, 190-195.

Sheng, J., Mao, J., Liu, F. and Hart, M. [2020]. A robust phase-only reflection full waveform inversion with multi-channel local correlation and dynamic minimum total-variation constraint. 82nd EAGE Annual Conference & Exhibition, *Extended Abstracts*.

Whitmore, N.D., Ramos-Martinez, J., Yang Y. and Valenciano, A.A. [2020]. Full wave field modeling with vector-reflectivity. 82nd EAGE Annual Conference & Exhibition*, Extended Abstracts.*

Yang, Y., Ramos-Martinez, J., Whitmore, D., Huang, G. and Chemingui, N. [2021]. Simultaneous inversion of velocity and reflectivity. *First Break*, **39**(12), 55-59.